ORIGINAL PAPER

Luminescent Donor-Acceptor β-Diketones: Modulation of Emission by Solvent Polarity and Group II Metal Binding

Guoqing Zhang · Shin Han Kim · Ruffin E. Evans · Byeong Hyo Kim · J. N. Demas · Cassandra L. Fraser

Abstract A class of aryl trifluoromethyl-containing β-diketones were synthesized via one step Claisen condensation. These π-conjugated diketones exhibit strong solvatochromism from intramolecular donor-acceptor charge transfer (CT). In addition, fluorescence quantum yields (ϕ_f) and lifetimes (τ_f) were measured in different solvents. Diketones exhibit bathochromic shifts in emission spectra with increasing solvent polarity. Fluorescence changes upon Group II metal binding were also studied. Despite the relatively simple structure, the anthracene-CF_3 diketone, atm, has strong binding affinity for Mg^{2+}. A 70 nm blue shift and sixfold increase in intensity were observed upon addition of only one equivalent $MgCl_2$ in ethanol solution. It also shows selectivity for Mg^{2+} binding even in the presence of excess Ca^{2+}. Association constant (K_a) calculations suggest atm has two orders of magnitude stronger chelation for divalent magnesium than for calcium. These findings make atm an attractive starting point for molecular probe and light emitting material design.

Keywords Fluorescent β-diketones · Anthracene · Naphthalene · Solvatochromism · Mg^{2+} and Ca^{2+} binding

Introduction

Donor-acceptor (D-A) systems [1] have been studied extensively for their optical properties and applications in chemical sensors [2]; photovoltaics [3], photodetectors [4], OLEDs [5] and non-linear optics [6]. Often their emission is polarity sensitive, given charge separation in the excited state. The optical properties of organic D-A molecules may also be modulated by metal binding. Typically metals inhibit photoinduced electron transfer (PET) from a donor moiety [2, 7]; however, fluorophores may also be altered by metal coordination to the acceptors [8].
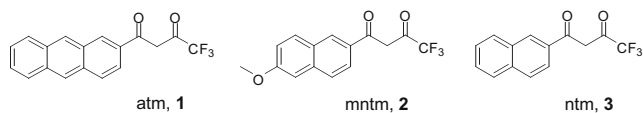
β-Diketonate acceptors, for example, are classic ligands for main group, transition metal and lanthanide series elements [9]. Their complexes display a vast array of chemical and physical functions ranging from light emission [10] to molecular recognition [11] and catalysis [12]. Our work with polymeric boron [13, 14], iron [15] and europium [16] complexes, for instance, features dibenzoyl-methane (dbm) ligands. Other reports have focused on diketone binding with Group II metals due to their importance in biology [17, 18]. For example, diketo acid derivatives serve as antiviral Mg^{2+}-chelate drug leads, given that Mg^{2+} is believed to be essential for the function of HIV integrase and hepatitis C polymerase in viral replication [19, 20]. Although many optical detection methods for Mg^{2+} and Ca^{2+} have been developed [21, 22], few involve diketone binding.

Here, we report the photophysical properties of a series of β-diketone D-A compounds containing an electron withdrawing $-CF_3$ substituent, anthroyltrifluoro acetyl-methane (atm, **1**), methoxynaphthoyl trifluoroacetylmethane (mntm, **2**) [23], and commercially available naphthoyl trifluoroacetylmethane (ntm, **3**). The naphthyl-CF_3 compound, **3**, has been employed as a photon-absorbing component in combination with lanthanide metals [23, 24]. The luminescence properties of **3** itself, however, have not drawn much attention perhaps because it is not such an impressive emitter ($\phi_f < 0.05$ in most solvents). This undoubt-edly precluded its use in many contexts, such as biology,

G. Zhang · R. E. Evans · J. N. Demas · C. L. Fraser (✉)
Department of Chemistry, University of Virginia,
Charlottesville, VA 22904, USA
e-mail: fraser@virginia.edu

S. H. Kim · B. H. Kim
Department of Chemistry, Kwangwoon University,
Seoul 139-701, Korea

where relatively strong emission is important for detection. Though the CF$_3$ group enhances the electron accepting ability of the diketone moeity, **3** lacks an electron donating substituent. The extent of conjugation (naphthalene vs. anthracene) in the aromatic spacer can also play an important role. The modulation of emission by solvent polarity and metal binding, namely Mg^{2+} and Ca^{2+}, are explored.

Experimental section

Materials Solvents THF, Toluene, EtOAc, CH$_2$Cl$_2$ and CH$_3$CN, were dried and purified by passage through alumina columns. All other reagents and solvents were used as received from Sigma-Aldrich without further purification.

Methods ^{1}H NMR (300 MHz) spectra were recorded on a UnityInova 300/51 instrument in CDCl$_3$ unless indicated otherwise. ^{1}H NMR spectra were referenced to the signal for residual protio chloroform at 7.26 ppm and coupling constants are given in hertz. Elemental analysis was performed by Atlantic Microlab, Inc., Norcross, GA. UV/Vis spectra were collected on a Hewlett-Packard 8452A diode-array spectrophotometer. Fluorescence emission spectra were recorded on a Horiba Fluorolog-3 Model FL3-22 spectrofluorometer (double-grating excitation and double-grating emission monochromator). Time-correlated single-photon counting (TCSPC) lifetime measurements were performed with a NanoLED-370 (369 nm) as the excitation source and DataStation Hub as the SPC controller. Lifetime data were analyzed with DataStation v2.4 software from Horiba Jobin Yvon.

1-(anthracen-2-yl)-4,4,4-trifluorobutane-1,3-dione (atm) (1) 2-Acetylanthracene (200 mg, 0.908 mmol) was added to a flame-dried 2-neck round bottom flask under nitrogen, and dissolved in THF (25 mL). A sodium hydride suspension (53.2 mg, 2.22 mmol) in THF (25 mL) was prepared in a 50 mL, flame-dried Schlenk flask. The NaH suspension was transferred to the two-neck round bottom flask via cannula followed by the addition of ethyl trifluoroacetate (258 mg, 220 μL, 1.81 mmol) via a 500 μL Hamilton syringe. The resulting reaction mixture was heated at reflux for 45 min, cooled to room temperature, and then further cooled in an ice bath. The reaction was quenched by dropwise addition of a saturated aqueous solution of sodium bicarbonate (5 mL) and then the pH of aqueous layer was adjusted to 6 with 3 M HCl.

The organic layer was removed *in vacuo* and the aqueous layer was extracted with CH$_2$Cl$_2$ (3×25 mL). The combined organic layers were dried over sodium sulfate and concentrated in vacuo to give a brown solid. The crude product was dissolved in acetone and recrystallized by slow addition of hexanes to give atm (**1**) as dark yellow crystals: 160 mg (56%). ^{1}H NMR (CDCl$_3$) δ 15.25 (s, 1H, COCH=CCF$_3$O*H*), 8.76 (s, 1H, 1′-Ar*H*), 8.62 (s, 1H, 9′-Ar*H*), 8.47 (s, 1H, 10′-Ar*H*), 8.06 (m, 3H, 3′,4′,8′-Ar*H*), 7.87 (d, *J* = 10.4, 1H, 5′-Ar*H*), 7.66 (m, 2H, 6′,7′-Ar*H*), 6.77 (s, 1*H*, COC*H*=CCF$_3$OH). ^{13}C NMR (CDCl$_3$) δ 185.8, 133.6, 132.7, 132.3, 131.2, 130.2, 129.6, 129.4, 129.3, 128.6, 128.2, 127.2, 126.5, 126.3, 121.4, 92.6. m.p.: 168–170 °C. Anal. calcd for C$_{18}$H$_{11}$F$_3$O$_2$: C, 68.36; H, 3.51. Found: C, 68.10; H, 3.49. UV/Vis (EtOH): λ$_1$=337 nm (ε=39,000 M^{-1} cm^{-1}), λ$_2$=423 nm (ε=7,600 M^{-1} cm^{-1}) [25].

4,4,4-trifluoro-1-(6-methoxynaphthalen-2-yl)butane-1,3-dione (mntm) (2) The mntm diketone was prepared as described for **1**: 6-methoxyl-2-acetylnaphthalene (401 mg, 2.00 mmol); NaH (108 mg, 4.52 mmol); CF$_3$COEt (568 mg, 480 μL, 4.00 mmol). The product **2** was obtained as fluorescent light green needles: 441 mg (74%). m.p. 90–92 °C ^{1}H NMR (CDCl$_3$) δ 15.37 (s, 1H, COCH=CCF$_3$O*H*), 8.46 (s, 1H, 1′-Ar*H*), 7.92 (d, *J* = 8.4, 1H, 3′-Ar*H*), 7.87 (d, *J* = 8.9, 1H, 8′-Ar*H*), 7.81 (d, *J* = 8.5, 1H, 4′-Ar*H*), 7.24 (d, *J* = 8.9, 1H, 7′-Ar*H*), 7.17 (s,1H, 5′-Ar*H*), 6.69 (s, 1H, COC*H*=CCF$_3$OH), 3.97 (s, 3H, C*H*$_3$OAr). ^{13}C NMR (CDCl$_3$) δ 182.2, 160.3, 137.8, 131.2, 129.4, 127.5, 123.5, 120.2, 105.8, 92.0, 55.4. Anal. calcd for C$_{15}$H$_{11}$F$_3$O$_3$: C, 60.82; H, 3.74. Found: C, 60.73; H, 3.71. UV/Vis (EtOH): λ$_{max}$ = 350 nm, ε = 18,000 M^{-1} cm^{-1}.

4,4,4-trifluoro-1-(naphthalen-2-yl)butane-1,3-dione (ntm) (3) The ntm diketone was used as received from Sigma-Alrich without further purification. ^{1}H NMR (CDCl$_3$) δ 15.26 (s, 1H, COCH=CCF$_3$O*H*), 8.53 (s, 1H, 1′-Ar*H*), 7.62 (m, 4H, 3′, 4′, 7′, 8′-Ar*H*), 7.24 (m, 2H, 5′, 6′-Ar*H*), 6.72 (s, 1H, COC*H*COCF$_3$). ^{13}C NMR (CDCl$_3$) δ 186.0, 135.9, 132.5, 129.9, 129.6, 129.1, 128.9, 127.8, 127.2, 122.7, 92.5. m.p. 74–76 °C.

Quantum yield measurements Fluorescence quantum yields, ϕ_f, for diketones **1**, **2**, and **3** in different solvents were measured under air versus quinine sulfate in 0.1 M H$_2$SO$_{4(aq)}$ as a standard, as previously described [See Ref. [29], Section II. C.2, equation 16] using the following values: ϕ_f quinine sulfate = 0.58, [26] n_D^{20} water = 1.333 n_D^{20} hexanes = 1.372 n_D^{20} toluene = 1.494, n_D^{20} EtOAc = 1.370, n_D^{20} CH$_2$Cl$_2$ = 1.424, n_D^{20}CH$_3$CN = 1.341 n_D^{20} EtOH = 1.360. Optically dilute solutions of **1**, **2** and **3** in the indicated solvents and an 0.1 M H$_2$SO$_4$ aqueous solution of the anthracene standard were prepared in 1 cm

Table 1 Fluorescence data for diketones **1**, **2** and **3**

	Solvent	λ_{em} (nm)	τ_{pw0} (ns)[a]	κ^2	ϕ_f^b
1	Hexanes	448	2.9[c]	1.13	0.31
	Toluene	490	7.9	1.18	0.32
	EtOAc	514	11.9	1.16	0.34
	CH_2Cl_2	535	13.1	1.02	0.52
	CH_3CN	557	11.2	1.18	0.11
	EtOH	561	5.5[d]	1.24	0.026
2	Hexanes	410	0.2[c]	1.17	0.0019
	Toluene	435	0.3	1.14	0.0012
	EtOAc	450	1.1	1.21	0.048
	CH_2Cl_2	459	1.2	1.09	0.12
	CH_3CN	477	2.7	1.11	0.21
	EtOH	486	2.0[d]	1.14	0.023
3	Hexanes	~400[e]	-[e]	-	0.0028
	Toluene	~420[e]	-[e]	-	0.0021
	EtOAc	437	0.3	1.26	0.0059
	CH_2Cl_2	443	0.4	1.12	0.016
	CH_3CN	460	2.6	1.20	0.020
	EtOH	479	4.2[d]	1.21	0.026

[a] Preexponential weighted lifetimes [28]. Data fit to double-exponential decay unless otherwise indicated, [b] Relative to quinine sulfate standard. (ϕ_f=0.58) in 0.1 M H_2SO_4 [26], [c] Single-exponential decay, [d] Triple-exponential decay, [e] Signal too weak to detect. See Fig. 2c

path length quartz cuvettes and absorbances (A ~ 0.05) were recorded using a Hewlett Packard 8452A UV/Vis spectrometer. Steady state emission spectra were obtained on a Horiba Fluorolog-3 Model FL3-22 spectrofluorometer (λ_{ex} = 350 nm; emission integration range: 365–700 nm).

Titration Absolute EtOH was purged with N_2 for ~20 min prior to use in the preparation of diketone, $MgCl_2$, and $CaCl_2$ solutions. An ethanol solution of **1** (3 mL, 50 µM) was prepared in a quartz fluorometer cell with a septum screw top (10 mm path, Starna Cells, Inc.) for acquisition of both absorption and emission spectra. Stock EtOH solutions of $MgCl_2$ and $CaCl_2$ (1.5 mM, i.e., 0.1 eq Mg^{2+}/**1** = 10 µL) were prepared for titration against the EtOH solution of **1** (same for **2** and **3**) via a Hamilton syringe. Both absorption and emission spectra were corrected with a volume dilution factor $V_{df} = 1+x/3000$. Titrations between **1** and $MgBr_2$ or $Mg(NO_3)_2$ were carried out under the same experimental condition.

Association constants Luminescence intensity and absorption titration spectra were fit to give association constants

$$M + L \overset{K_a}{\rightleftarrows} ML \qquad (1)$$

where M is the metal and L is the ligand. Emission intensities and absorbances, Bs, at individual wavelengths are given by

$$B([M]) = B_L f_L([M]) + B_{ML} f_{ML}([M]) \qquad (2)$$

$$f_{ML}([M]) = [1 + K_a[L] + K_a[M] - D^{1/2}]/(2K_aL) \qquad (3)$$
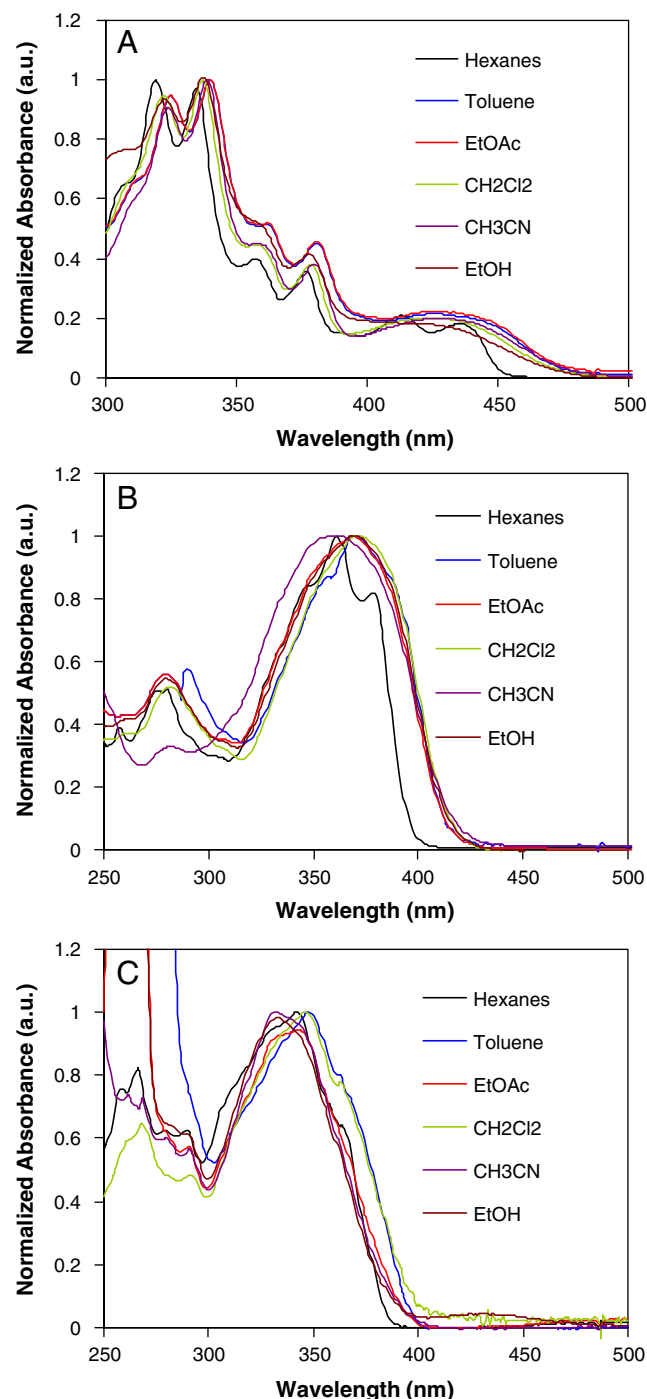

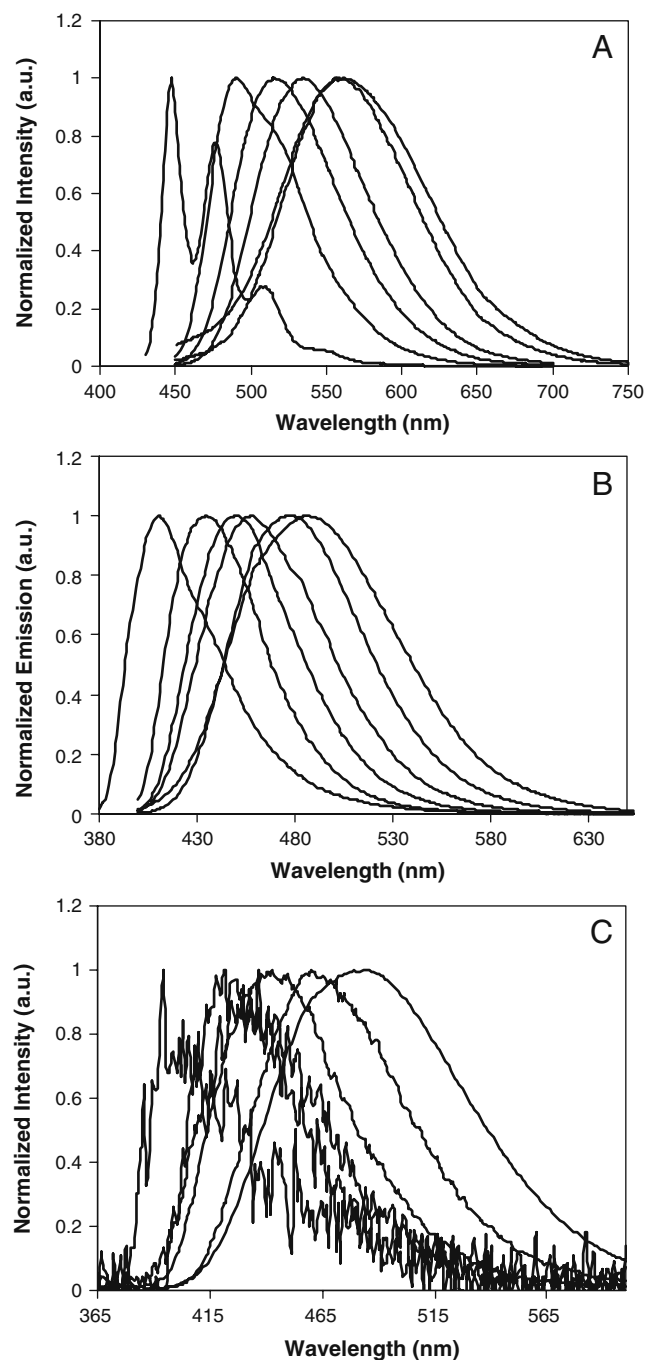**Fig. 1** Absorption spectra of atm **1** (**a**), mntm **2** (**b**) and ntm **3** (**c**) in the indicated solvents

Fig. 2 Emission spectra of **1** (**a**), **2** (**b**) and **3** (**c**) in different solvents (*left* to *right*: hexanes, toluene, EtOAc, CH$_2$Cl$_2$, CH$_3$CN, EtOH)

$$D = 1 + 2K_a[L] + 2K_a[M] + K_a^2[L]^2 - 2K_a^2[L][M]$$
$$+ K_a^2[M]^2 \tag{4}$$

$$f_L([M]) = 1 - f_{ML}([M]) \tag{5}$$

where f_L and f_{ML} are the fraction of the ligand present as free L and ML respectively. [M] and [L] are the total metal

and ligand concentrations in all chemical forms. In the titrations the ligand concentration was fixed at 50 μM. Absorption data were fit at 432 nm and the emission data at 482 nm (Mg^{2+}) or 485 nm (Ca^{2+}). The intensity or absorbance data were fit to Eq. 1 by nonlinear least squares using PSI-Plot (Pearl River, NY). Full details of the fits are provided in the Supporting Information.

The alternative fitting procedure used OlisSpectralWorks global fitting software (Olis, Inc., Bogart, GA) where all wavelengths were fit simultaneously to the same model with a fixed K$_a$. Singular value decomposition was used to find the primary components in the data, and then the data set was reconstructed using these two components. The reconstituted spectra were then fit globally by nonlinear least squares to the equilibrium model of Eq. 2–5. Two principal components were used in the fit, although there was evidence for contribution from a third component.
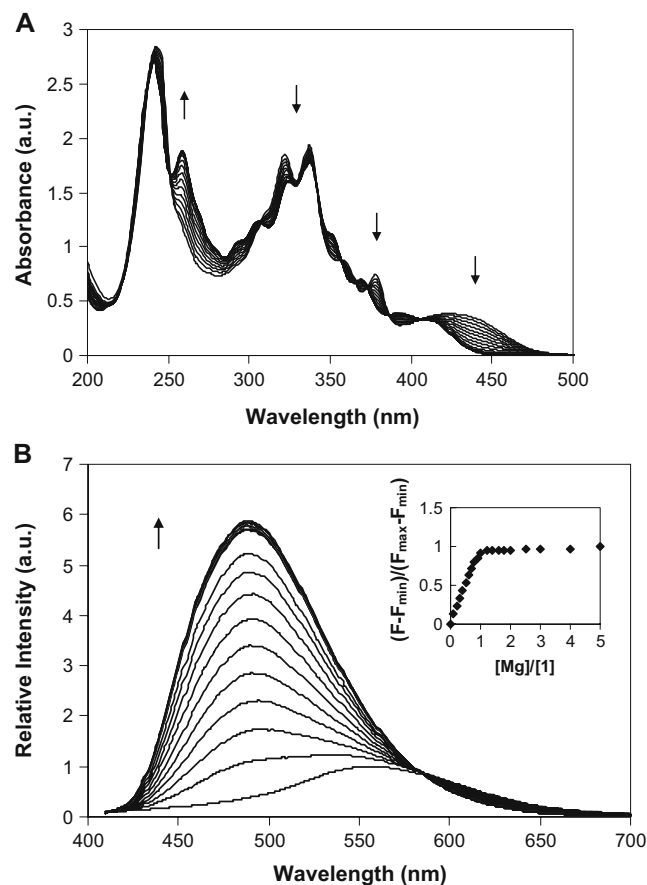
Fig. 3 UV/Vis absorption (**a**) and fluorescence emission (**b**) spectral changes upon addition of MgCl$_2$ (0.1, 0.2, 0.3, 0.4, 0.5, 0.6, 0.7, 0.8, 0.9, 1.0, 1.2, 1.4, 1.6, 1.8, 2.0, 2.5, 3.0, 4.0, 5.0 equiv) to diketone **1** in EtOH (3 mL, 50 μM). Inset: Relationship between fluorescence intensity change and Mg^{2+}/**1** ratio at 491 nm. F$_{min}$: ligand fluorescence intensity at 491 nm; F$_{max}$: fluorescence intensity at 491 nm in the presence of 5 equiv of MgCl$_2$; F: variable fluorescence intensity at 491 nm

Table 2 Fluorescence lifetime data for diketone **1** and **2** with weighting factors

	Hexanes	Toluene	EtOAc	CH_2Cl_2	CH_3CN	EtOH
1	2.9[a] (100%)[b]	5.6 (39%)	9.0 (40%)	10.9 (48%)	9.5 (11%)	1.7 (22%)
		9.4 (61%)	13.9 (60%)	15.3 (52%)	11.4 (89%)	3.8 (60%)
						16.9 (18%)
2	0.2 (100%)	0.2 (51%)	0.5 (32%)	0.6 (67%)	1.1 (23%)	0.9 (11%)
		0.4 (49%)	1.4 (68%)	2.5 (33%)	3.2 (77%)	2.1 (87%)
						3.7 (2%)

[a] lifetime (ns), [b] preexponential weighting percentage

Results and discussion

To test donor, acceptor and arene effects on optical properties, diketones **1** and **2** were prepared via one-step Claisen condensation in NaH/THF [15] and their absorption, emission, and optical response after Group II binding were investigated. Optical properties of diketones **1–3** were explored in solvents of varying polarity (Table 1). Both absorption (Fig. 1) and emission (Fig. 2) spectra for **1**, are highly structured in non-polar hexanes but are broad and red shifted in more polar solvents. The subtle differences in absorption spectra and dramatic bathochromic shift (113 nm) in emission spectra with increasing solvent polarity suggest that the dipole moment increases in the excited state [27]. Similar trends in absorption and emission have been noted for **2** and **3** in solvents of varying polarity (Figs. 1 and 2). The color ranges for mntm (75 nm) and ntm (~80 nm) are less dramatic than for **1**, possibly because naphthalene is a weaker donor than anthracene. As is clearly evident in Fig. 2C given the considerable noise in the normalized spectra, emission intensities for **3** in non-polar solvents are very low.

Ihemels et al. [30–32] have also reported a series of fluorescent dyes with D-A structures featuring D = 6-methoxyanthracene and A = ester, amide, oxazoline, or N-acyl urea derivatives. Compared to their systems, synthetically more accessible **1** shows a wider bathochromic shift range (113 nm) with solvent polarity. This polarity dependence is likely to be influenced by both negative and positive "solvatokinetic effects" [33], where the former is the increase in ϕ_f with an enhancement of intramolecular charge transfer (ICT) and the latter is the reduction of ϕ_f when the ICT state is too close to the triplet which promotes intersystem crossing or nonradiative decay to the ground state, as explained by the energy gap law.

The radiative decays of **1–3** can be fit to single, double or triple exponentials depending on the solvent polarity, and trends in lifetime values parallel quantum yields (Tables 1 and 2). The dynamics are especially complex in polar protic solvents such as ethanol where triple exponential decay is observed. Along with the possibility of mixed emission from both locally excited and ICT states [24], emission spectra may also be affected by hydrogen bonding which is known to affect the keto enol equilibrium [34, 35]. Fluorescence lifetimes for naphthyl diketones **2** and **3** are considerably shorter than for **1**.

β-Diketone emission can also be modulated by metal binding [8]. A titration was performed to study magnesium binding to the anthracene diketone **1** (Fig. 3). Binding studies were performed for **1**, given more dramatic spectral shifts than for **2** and **3**. The reaction was run in ethanol because **1** is not soluble in water. Because the Mg^{2+} salts are hygroscopic, reactions were run under nitrogen using dry solvent, given that water could serve as a ligand and affect spectroscopic properties. Upon Mg^{2+} addition, the absorption in the visible region (400–450 nm) gradually decreases, accompanied by a distinct new feature at ~250 nm indicating coordination. The diminished absorbance at longer wavelength may imply a weaker CT state for the new Mg^{2+} atm complex. The emission and absorption exhibited isosbestic or isoemissive points up to
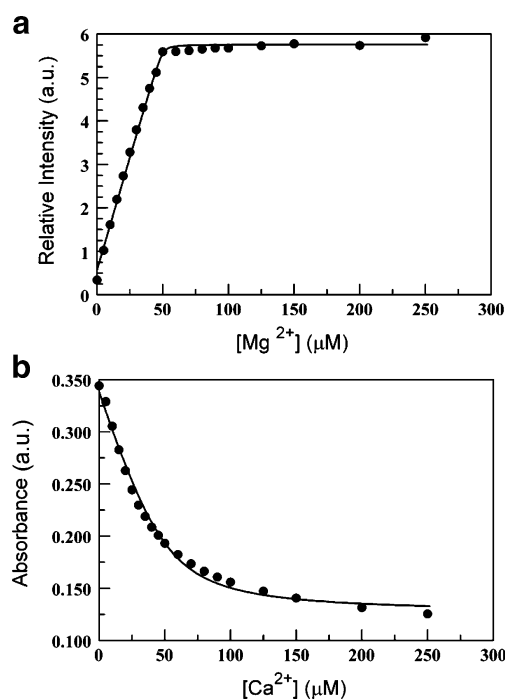

Fig. 4 Emission titration curves for Mg^{2+} with **1** at 482 nm (**a**) and absorption titration for Ca^{2+} at 432 nm (**b**) in ethanol. The *solid lines* are the best fits to a 1:1 binding

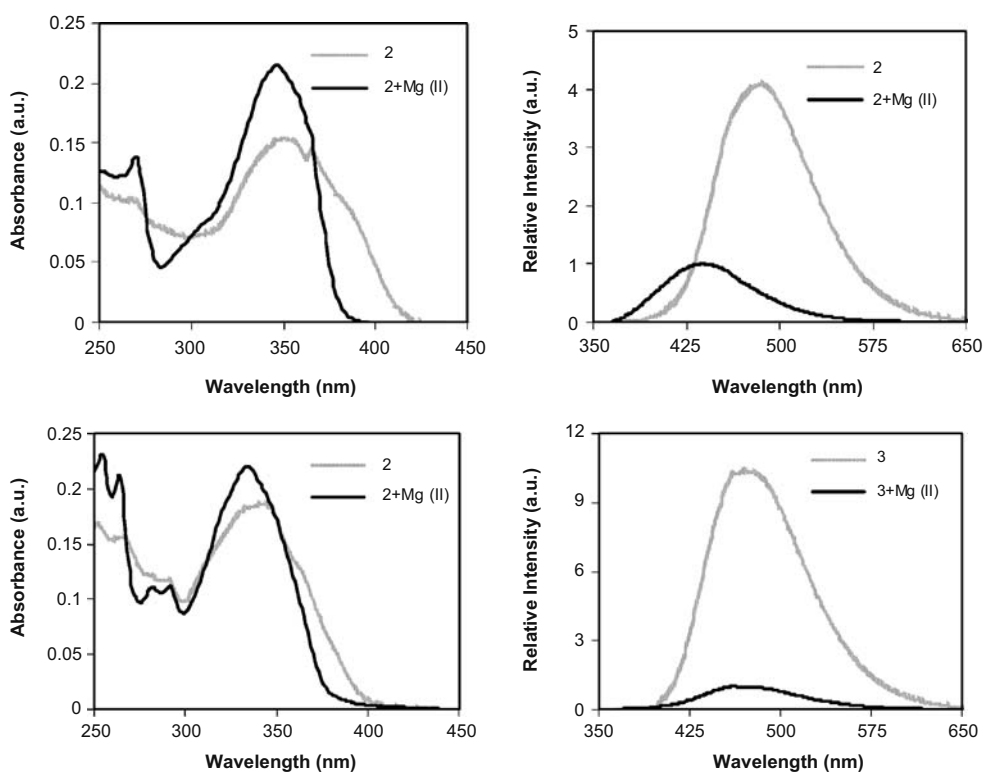**Table 3** Association constants for metal ion binding to **1** with global and single wavelength fitting

	Method	K_a Global (μM^{-1})	K_a Single λ (μM^{-1})
Mg^{2+}	absorption	6 ± 3	9 ± 3
	emission	10 ± 10	12 ± 12
Ca^{2+}	absorption	$0.11\pm.01$	0.13 ± 0.02
	emission	0.10 ± 0.01	0.11 ± 0.02

about one equivalent of MgCl$_2$ (Fig. 3). Beyond that the absorption spectrum changed slowly and the absorption isosbestic and isoemissive points began to shift and were lost. This indicates a tight 1:1 binding between Mg^{2+} and **1** in EtOH solution along with a much weaker 1:2 binding. The best fit to the emission data at 432 nm with a 1:1 binding model is shown in Fig. 4a. This is consistent with known 1:1 [36] and 1:2 [37] binding for Mg^{2+} and β-diketones. For example, reaction of Mg metal with diketones gives a bis complex [37] but in ethanol, the solvent may act as an auxiliary ligand for Mg^{2+} [38]. It is clear here that up to about the equivalence point the mono complex is the predominant species. The K$_a$s for 1:1 binding derived by the single wavelength titration curves and the multiwavelength fits are given in Table 3. The standard deviation is provided for each measurement. There is a good agreement between the two methods. The large uncertainties on the Mg^{2+} data are due to the high concentration of metal. Only the small curvature near the

end point provides any information on the binding constant. It is not our intent to provide rigorous values for the association constants, especially since we are ignoring the 1:2 binding at higher concentrations. Our data do, however, show the strong preference of **1** for Mg^{2+} over Ca^{2+} and provide an estimate of the sensitivity of **1** for Mg^{2+}.

The Mg^{2+}-**1** complex has a significantly blue-shifted emission (491 nm) compared to diketone ligand **1** (561 nm) and the quantum yield of the titration solution showed a ten-fold increase over the diketone ligand (0.026 to 0.26 after 5 equiv MgCl$_2$ added) and a slight increase in lifetime (5.5 ns to 6.7 ns). An enhanced fluorescence response at a blue-shifted wavelength is usually preferred for signal detection. This is because most fluorescent molecules have long emission tails that could interfere with red-shifted spectral changes. This blue shift method has been described by Swager et al. as "dark-field detection" [39]. In addition, **1** exhibits good sensitivity for Mg^{2+} since the emission spectrum is perceivably different even after addition of only 0.1 equiv of metal. From the association constant, detection would be at the 100 nM level or less. To examine counterion effects, titrations of ethanol soluble MgBr$_2$ and Mg(NO$_3$)$_2$ salts were also performed. Both absorption and emission responses were independent of the counterions.

Reactions of naphthyl diketones **2** and **3** with 1 equiv MgCl$_2$ in EtOH were also tested (Fig. 5). In the UV/Vis spectra, the absorbance at longer wavelength diminishes and a higher energy peak increases. In contrast to **1** where the fluorescence intensity increases upon Mg^{2+} binding, for

Fig. 5 UV/Vis absorption and fluorescence emission spectra of **2** and **3** (10 μM in EtOH) and their responses to the addition of 1 equiv MgCl$_2$
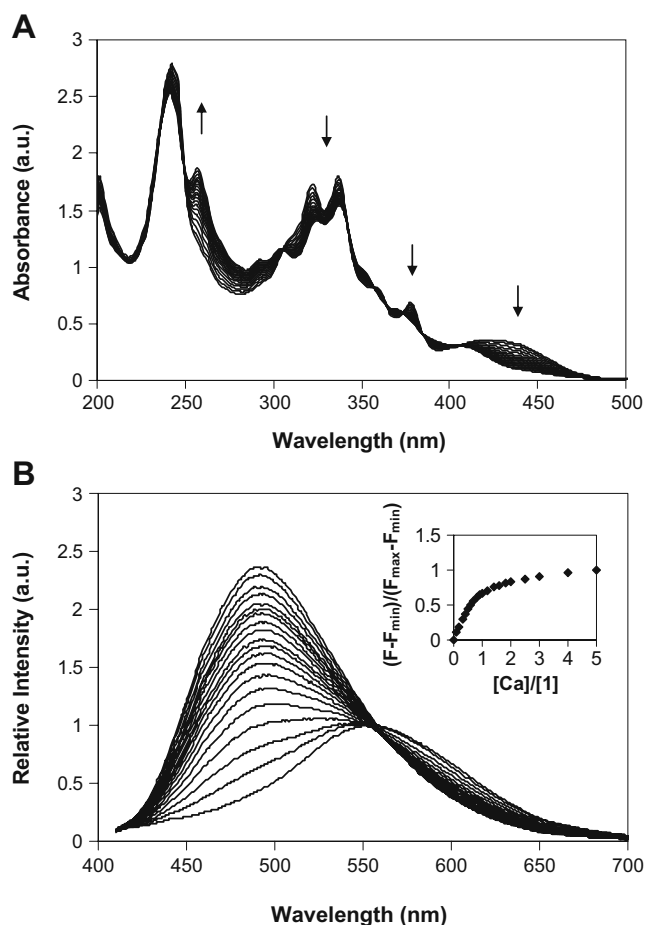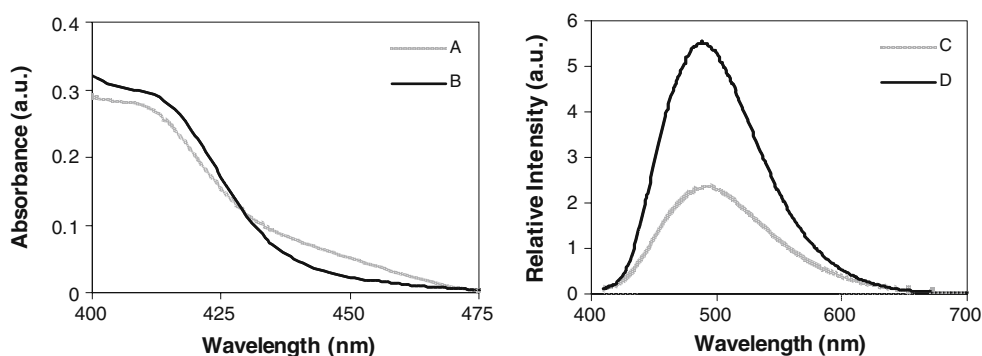
Fig. 6 UV/Vis absorption (**a**) and fluorescence emission (**b**) spectral changes upon addition of CaCl$_2$ (0.1, 0.2, 0.3, 0.4, 0.5, 0.6, 0.7, 0.8, 0.9, 1.0, 1.2, 1.4, 1.6, 1.8, 2.0, 2.5, 3.0, 4.0, 5.0 equiv) to diketone **1** in EtOH (3 mL, 50 µM). Inset: Relationship between fluorescence intensity change and [Ca^{2+}]/[**1**] ratio at 495 nm. F$_{min}$: ligand fluorescence intensity at 495 nm; F$_{max}$: fluorescence intensity at 495 nm in the presence of 5 equiv CaCl$_2$; F: variable fluorescence intensity at 495 nm

2 and **3** the intensity of the Mg^{2+} complexes decreases relative to the free ligands (i.e. ~4 and ~11 times less than **2** and **3** respectively). For **1** and **2**, there is little to no residual signal arising from the diketone ligand, however for **3** the total emission could be arising mainly from the

ligand. The change in fluorescence upon Mg^{2+} binding was also studied by Sato et al. [36] for a D-A diketone N, N′-4-amino-4′-cyanodibenzoylmethane. They reported a small blue shift in emission (~10 nm) and a roughly four fold fluorescence enhancement (ϕ_f increase from 0.00016 to 0.00068) after addition of 1,000 equiv Mg^{2+} (10 mM). Compared to their naphthyl and benzyl systems, the results for the anthracene diketone **1** are quite impressive—a ~70 nm blue shift and tenfold increase in quantum yield after addition of only 1 equiv of magnesium.

For comparison, the titration of diketone **1** with CaCl$_2$, a chemically similar biological relevant metal, was also investigated (Fig. 6). Again, up to about a [Ca^{2+}]/[**1**] ratio of one there are good isosbestic and isoemissive points, which begin to degrade at higher [Ca^{2+}]. This is similar to the Mg^{2+} system where the 1:1 binding is substantially tighter than the 1:2 binding. However, the Ca^{2+} binding is much weaker than for Mg^{2+}, as shown by the fact that the longer wavelength ligand absorption (~475 nm) is present even after addition of 5 equiv CaCl$_2$. This weaker binding is demonstrated by the fitting of the 1:1 model to the absorbance at 432 nm (Fig. 4b). The emission maximum for the Ca^{2+} complex also shows a significant blue shift (**1**: 561 nm vs Ca−**1**: 495 nm) at 1:1 loading. However, the fluorescence change upon Ca^{2+} binding is different. First, at 1 equiv of CaCl$_2$, the intensity only doubles compared to a sixfold increase for MgCl$_2$. Secondly, the peak intensity does not plateau at 1 equiv, but instead continues to increase gradually even after 5 equiv of Ca^{2+} have been added. This clearly shows weaker binding for Ca^{2+} than for Mg^{2+}. This is consistent with the observed two order of magnitude stronger binding of related acetylacetone to Mg^{2+} over Ca^{2+} in water-dioxane [40]. K$_a$s for a 1:1 binding model are given in Table 3 and confirm the magnitude of the difference. The systematic deviations, especially at higher concentrations, indicates the presence of a weaker 1:2 binding. In a competition experiment, when 1 equiv of Mg^{2+} was added to the 5:1 Ca^{2+}−**1** mixture, both absorption and emission spectra show features that are characteristic of the Mg^{2+}−**1** complex, with a corresponding six fold emission intensity increase at 491 nm (Fig. 7). This

Fig. 7 UV/Vis absorption and fluorescence emission spectral changes upon addition of 1 equiv of MgCl$_2$ (**b**, **d**) to a 5:1 CaCl$_2$:1 (**a**, **c**) ethanol solution (50 µM)

too, indicates preferential binding of the anthracene diketone ligand to Mg^{2+} even in the presence of excess Ca^{2+}. The high sensitivity to magnesium binding, blue-shifted emission, counterion independence, and Mg^{2+} selectivity make **1** a good starting point for sensor design.

Conclusion

In summary, the photophysical properties of luminescent D-A β-diketones were investigated. Fluorescence spectra for **1–3** show strong solvent polarity dependence. Spectroscopic responses to Mg^{2+} and Ca^{2+} vary for the ligands, with diketone **1** showing selective binding for Mg^{2+} in the presence of Ca^{2+} and a hypsochromic shift accompanied by enhanced fluorescence emission. These features of simple, synthetically accessible naphthylene- and anthracene-CF_3 diketones make them good lead compounds for optical polarity probes, metal sensors and chemically tunable additives for luminescent materials applications.

References

1. Grabowski ZR, Rotkiewicz K, Rettig W (2003) Structural changes accompanying intramolecular electron transfer: focus on twisted intramolecular charge-transfer states and structures. Chem Rev 103:3899–4032. doi:10.1021/cr9407451

2. de Silva AP, Gunaratne HQN, Gunnlaugsson T, Huxley AJM, McCoy CP, Rademacher JT, Rice TE (1997) Signalling recognition events with fluorescent sensors and switches. Chem Rev 97:1515–1566. doi:10.1021/cr960386p

3. Yu G, Gao J, Hummelen JC, Wudl F, Heeger AJ (1995) Polymer photovoltaic cells: enhanced efficiencies via a network of internal donor-acceptor heterojunctions. Science 270:1789–1791. doi:10.1126/science.270.5243.1789

4. Peumans P, Bulović V, Forrest SR (2000) Efficient high-bandwidth organic multilayer photodetectors. Appl Phys Lett 76:3855–3857. doi:10.1063/1.126800

5. Burrows PE, Shen Z, Bulović V, McCarty DM, Forrest SR, Cronin JA, Thompson ME (1996) Relationship between electroluminescence and current transport in organic heterojunction light-emitting devices. J Appl Phys 79:7991–8006. doi:10.1063/1.362350

6. Meyers F, Marder SR, Pierce BM, Bredas JL (1994) Electric field modulated nonlinear optical properties of donor-acceptor polyenes: sum-over-states investigation of the relationship between molecular polarizabilities (alpha, beta, and gamma) and bond length alternation. J Am Chem Soc 116:10703–10714. doi:10.1021/ja00102a040

7. Desvergne JP, Czarnik AW (1997) Chemosensors of ion and molecule recognition. Springer, London

8. Fery–Forgues S, Lavabre D, Rochal AD (1998) Strong interaction between a fluorescent β-diketone derivative and alkali and alkaline earth cations in solution studied by spectrophotometry. N J Chem 22:1531–1538. doi:10.1039/a802688b

9. Pettinari C, Marchetti F, Drozdov A (2003) β-Diketones and related ligands. Coord Chem Rev II 1:97–115

10. DeOliveira E, Neri CR, Serra OA, Prado AGS (2007) Antenna effect in highly luminescent Eu3+ anchored in hexagonal mesoporous silica. Chem Mater 19:5437–5442. doi:10.1021/cm701997y

11. Banet P, Legagneux L, Hesemann P, Moreau JJE, Nicole L, Quach A, Sanchez C, Tran-Thi TH (2008) Hybrid mesostructured thin films functionalized with DBM as new selective sensors of BF3. Sens Actuators B Chem 130:1–8. doi:10.1016/j.snb.2007.07.103

12. Huang W, Wang J, Shen Q, Zhou X (2007) An efficient Yb(OTf)3 catalyzed alkylation of 1, 3-dicarbonyl compounds using alcohols as substrates. Tetrahedron Lett 48:3969–3973. doi:10.1016/j.tetlet.2007.04.047

13. Zhang G, Chen J, Payne SJ, Kooi SE, Demas JN, Fraser CL (2007) Multi-emissive difluoroboron dibenzoylmethane polylactide exhibiting intense fluorescence and oxygen-sensitive room-temperature phosphorescence. J Am Chem Soc 129:8942–8943. doi:10.1021/ja0720255

14. Pfister A, Zhang G, Zareno J, Horwitz AF, Fraser CL (2008) Boron polylactide nanoparticles exhibiting fluorescence and phosphorescence in aqueous medium. ACS Nano 2:1252–1258. doi:10.1021/nn7003525

15. Gorczynski JL, Chen J, Fraser CL (2005) Iron tris(dibenzoyl-methane)-centered polylactide stars: Multiple roles for the metal complex in lactide ring-opening polymerization. J Am Chem Soc 127:14956–14957. doi:10.1021/ja0530927

16. Bender JL, Corbin PS, Fraser CL, Metcalf DH, Richardson FS, Thomas EL, Urbas AM (2002) Site-isolated luminescent europium complexes with polyester macroligands: Metal-centered heteroarm stars and nanoscale assemblies with labile block junctions. J Am Chem Soc 124:8526–8527. doi:10.1021/ja0261269

17. Cowan JA (1995) Biological chemistry of magnesium. VCH, New York

18. Berridge MJ, Bootman MD, Roderick HL (2003) Calcium signalling: dynamics, homeostasis and remodelling. Nat Rev Mol Cell Biol 4:517–529. doi:10.1038/nrm1155

19. Goldschmidt V, Didierjean J, Ehresmann B, Ehresmann C, Isel C, Marquet R (2006) Mg2+ dependency of HIV-1 reverse transcription, inhibition by nucleoside analogues and resistance. Nucleic Acids Res 34:42–52. doi:10.1093/nar/gkj411

20. Kirschberg T, Parrish J (2007) Metal chelators as antiviral agents. Curr Opin Drug Discov Devel 10:460–472

21. Park EJ, Brasuel M, Behrend C, Philbert MA, Kopelman R (2003) Ratiometric optical PEBBLE nanosensors for real-time magnesium ion concentrations inside viable cells. Anal Chem 75:3784–3791. doi:10.1021/ac0342323

22. Rudolf R, Mongillo M, Rizzuto R, Pozzan T (2003) Innovation: looking forward to seeing calcium. Nat Rev Mol Cell Biol 4:579–586. doi:10.1038/nrm1153

23. Uekawa M, Miyamoto Y, Ikeda H, Kaifu K, Nakaya T (1997) Synthesis and luminescent properties of europium complexes. Synth Met 91:259–262. doi:10.1016/S0379-6779(97)04027-7

24. Li Y, Yan B, Yang H (2008) Construction, characterization, and photoluminescence of mesoporous hybrids containing europium(III) complexes covalently bonded to SBA-15 directly functionalized by modified β-diketone. J Phys Chem C 112:3959–3968. doi:10.1021/jp710023q

25. λ1: anthracene moiety absorption maximum; λ2: charge-transfer band maximum

26. Lakowicz JR (2006) Principles of fluorescence spectroscopy, 3rd edn. Springer, New York, p 54

27. Kawski A (1992) Progress in photochemistry and photophysics. In: Rabek F (ed). CRC, Boca Raton, pp. 1–47

28. Carraway ER, Demas JN, DeGraff BA (1991) Photophysics and photochemistry of oxygen sensors based on luminescent transition metal complexes. Anal Chem 63:332–336. doi:10.1021/ac00004a006

29. Crosby GA, Demas JN (1971) The measurement of photo-luminescence quantum yields. J Phys Chem 75:991–1024. doi:10.1021/j100678a001

30. Bohne C, Ihmels H, Waidelich M, Yihwa C (2005) N-acylureido functionality as acceptor substituent in solvatochromic fluorescence probes: Detection of carboxylic acids, alcohols, and fluoride ions. J Am Chem Soc 127:17158–17159. doi:10.1021/ja052262c

31. Ihmels H, Meiswinkel A, Mohrschladt CJ, Otto D, Waidelich M, Towler M, White R, Albrecht M, Schnurpfeil A (2005) Anthryl-substituted heterocycles as acid-sensitive fluorescence probes. J Org Chem 70:3929–3938. doi:10.1021/jo047841z

32. Ihmels H, Meiswinkel A, Mohrschladt C (2002) Novel fluorescence probes based on 2, 6-donor-acceptor-substituted anthracene derivatives. J Org Lett 2:2865–2868. doi:10.1021/ol006291y

33. Wang P, Wu S (1995) Spectroscopy and photophysics of bridged enone derivatives: effect of molecular structure and solvent. J Photochem Photobiol Chem 86:109–113. doi:10.1016/1010-6030(94)03921-G

34. Iglesias E (1996) Enolization of benzoylacetone in aqueous surfactant solutions: A novel method for determining enolization constants. J Phys Chem 100:12592–12599. doi:10.1021/jp96047 3l

35. Iglesias E (1997) Determination of keto–enol equilibrium constants and the kinetic study of the nitrosation reaction of β-dicarbonyl compounds. J Chem Soc Perkin Trans 2:431–440. doi:10.1039/a607039f

36. Sato Y, Morimoto M, Segawa H, Shimidzu T (1995) Twisted intramolecular charge-transfer state of a donor-acceptor molecular system with a β-diketone bridge: tuning of emission through structural restriction by metal cation coordination. J Phys Chem 99:35–39. doi:10.1021/j100001a007

37. Hatch LF, Sutherland G (1948) Certain metal derivatives of 2, 4-pentanedione. J Org Chem 13:249–253. doi:10.1021/jo01160a012

38. Bertrand JA, Caine D (1964) Preparation and properties of methoxo complexes of divalent metal ions. J Am Chem Soc 86:2298–2299. doi:10.1021/ja01065a048

39. Thomas SW III, Venkatesan K, Muller P, Swager TM (2006) Dark-field oxidative addition-based chemosensing : New bis-cyclometalated Pt(II) complexes and phosphorescent detection of cyanogen halides. J Am Chem Soc 128:16641–16648. doi:10.1021/ja065645z

40. Van Ujtert LG (1983) Chelate compound stability constant calculations on metal diketonate complexes. Polyhedron 2:285–269. doi:10.1016/S0277-5387(00)83915-7